Paste Extrusion of Polytetrafluoroethylene (PTFE) Powders Through Tubular and Annular Dies at High Reduction Ratios

Pramod D. Patil,[1] Ochoa Isaias,[1] Christos Stamboulides,[1] Savvas G. Hatzikiriakos,[1] Fabio Polastri,[2] Valerj Kapeliouchko[2]

[1]*Department of Chemical and Biological Engineering, The University of British Columbia, Vancouver, BC, Canada*
[2]*Solvay Solexis S.P.A, Bolate, Milan, Italy*

Received 19 February 2007; accepted 30 September 2007
DOI 10.1002/app.27681
Published online 22 January 2008 in Wiley InterScience (www.interscience.wiley.com).

ABSTRACT: Paste extrusion experiments are reported for three different polytetrafluoroethylene (PTFE) fine powders using both capillary and annular dies having a high reduction ratio (cross-sectional area of reservoir to cross-sectional area of die at the exit) varied from 1000 up to 4000. The extrusion pressure is reported as a function of the apparent shear rate for various resins and dies. The approximate mathematical model for paste extrusion through capillary dies developed by Ariawan et al. (Ariawan et al., Can Chem Eng J, 2002, 80, 1153) was used to describe the experimental data by best fitting the five material constants of the constitutive model. Using these constants, the model developed by Patil et al. (Patil et al., AIChE J., 2006, 52, 4028) was used to predict the extrusion pressure for all three resins in annular dies. The model predictions are found to be consistent with experimental results and the analogy between the rod and tube extrusion models is demonstrated. © 2008 Wiley Periodicals, Inc. J Appl Polym Sci 108: 1055–1063, 2008

Key words: polytetrafluoroethylene; paste flow; tube extrusion; rod extrusion; radial flow hypothesis, annular die

INTRODUCTION

In polytetrafluoroethylene (PTFE) paste extrusion, fine powder of individual primary particles of diameter about 0.20–0.25 μm is first mixed with a lubricating liquid (lube) to form a paste.[1,2] The paste is consequently compacted at a typical pressure of 2 MPa to produce a preform of cylindrical shape that is nearly free of air voids. The next step involves loading the cylindrical preform into a ram extruder at a temperature slightly above 30°C where PTFE particles become reasonably deformable.[2] Extrusion through annular or capillary dies produces strong extrudates due to the structure formation through fibrillation of individual particles. This is usually followed by the evaporation of the lubricant by passing the extrudates through an oven. Sintering at high temperatures (380°C) is necessary when full strength and porosity elimination are required for processes such as wire coating and tube fabrication.[2–4]

Numerous constitutive models have been developed for flows of viscoelastic materials, such as polymer melts,[5] solids under plastic deformations,[6] and elastic–plastic materials that exhibit strain hardening as in the case of metal forming or wire drawing.[7] The empirical equation suggested by Benbow and Bridgwater[3] has been proven to be a good model; however, it cannot predict the effect of die entrance angle on the extrusion pressure of PTFE paste, although it works quite well for other pasty materials.[8–11] Because of its empirical nature, modifications of any theoretical significance are also difficult to incorporate. An improved analytical model for orifice extrusion of visco-plastic materials has recently been proposed.[12] Because of structure formation (fibrillation), strain hardening effects are obtained at high contraction angles during PTFE flow and, therefore, these models (Benbow and Bridgwater[3] and Basterfield et al.[12]) are not suitable for PTFE paste flow through cylindrical and annular dies.

Ariawan et al.[4] have proposed a visco-plastic model to predict the dependence of extrusion pressure on die geometrical parameters for rod extrusion. This approximate model successfully captures the nonmonotonic dependence of extrusion pressure on die entrance angle and other geometrical characteristics of the cylindrical die. Its derivation is based

Correspondence to: S. G. Hatzikiriakos (hatzikir@interchange.ubc.ca).
Contract grant sponsor: Solvay Solexis, Bollate Milan, Italy.

Journal of Applied Polymer Science, Vol. 108, 1055–1063 (2008)

on the radial flow hypothesis (RFH), whose validity has been demonstrated experimentally.[4,13] Although this model does not explicitly predict micromechanical details of the extrudates, it describes the extrusion pressure as a function of the geometrical parameters of cylindrical dies very well and, therefore, is very useful in die design.[4] A similar approach has been adopted by Patil et al.[14] to propose a model for the dependence of extrusion pressure in tube extrusion (annular flow).

The main objective of the present work is to demonstrate the consistency of the two models in describing PTFE paste extrusion through both capillary and annular dies. Experiments are performed using various PTFE powders and a variety of capillary and annular dies having various geometrical characteristics. The material constants are determined from capillary extrusion experiments and consequently are used to predict the extrusion pressure in annular flow. The consistency between the model predictions and the experimental results and between the two models is demonstrated.

The organization of this article is as follows. First, the two models for capillary and annular PTFE paste flow are presented. The experimental results for three PTFE powders are presented in detail using both capillary and annular dies. Then, the experimental results are compared with the two models in a way described earlier to demonstrate their consistency. Finally, a short summary of the results concludes the article.

MATERIAL AND EXPERIMENTAL PROCEDURES

Materials

Three different PTFE fine powder resins were used to compare their performance in paste extrusion. These are listed in Table I along with some physical properties such as density and particle size. All three of them are copolymers (resin A and B contain the same comonomer) with A to be of higher molecular weight compared to B.

The lubricant used to prepare the pastes was Isopar® K obtained from ExxonMobil and used as received without any further purification. This lubricant is a colorless isoparaffinic fluid, with a surface tension of 0.0259 N/m, density of 760 kg/m^3, and viscosity of 0.00139 Pa s, at room temperature.

TABLE I
PTFE Powders Used in this Work

Sample	Comonomer	SSG	Bulk density	D50
A	PFMD/PFP	2.166	450	577
B	PFMD/PFP	2.162	460	634
C	PFP	2.164	454	637

PFMD, perfluoromethoxydioxole; PFP, perfluoropropene; D50 is the particles' dimension at which 50% of the powder is below and 50% is above.

Paste preparation

The PTFE pastes were prepared as follows. First, the fine powder was mixed slowly with the appropriate amount of the processing aid to produce a paste of 18 wt % (38.8 vol %) in lubricant. Consequently, the paste was continued to be mixed in a thoroughly sealed rotating jar mill at low speed for a few hours. Finally, before testing, the paste was aged for 24 h at room temperature in a sealed jar to avoid lubricant evaporation.

Experimental procedure

A Universal Testing Machine (UTM) was used for both the preforming and extrusion experiments. The UTM comprised of a load cell of capacity 222,687 N (maximum load) attached to a motor driven cross head. After the preparation, the paste was preformed into a cylindrical billet by first placing it into a barrel of diameter equal to 2.54 cm with four heating zones to keep the temperature uniform. A blank die was used for the preforming stage. A pressure of 2 MPa was applied for 30 s to remove the air voids and to produce a cylindrical billet of good dimensional stability. It has been concluded from previous studies that such conditions can remove the air and significantly reduce the voids from the paste.[4,14–16]

Upon the completion of preforming, the blank die was replaced either by a cylindrical die or an annular die and extrusion then proceeded at various piston speeds that resulted into different shear rates. All extrusion experiments were carried out at the temperature of 35°C. After the extrusion experiments, extrudates were collected and dried at 100–120°C under vacuum for about 24 h for further examination i.e. mechanical properties are of no concern in the present article.

Dies used

The capillary (cylindrical) dies used for extrusion were all made of stainless steel. The entrance angle of all dies used was 40°. Dies having various length-to-diameter ratios, L/D_a, were also used to assess the effect of L/D_a; dies having L/D_a = 0, 5, 10, 20, and 30 were constructed for this purpose. In this work, the effect of the high reduction ratio on the extrusion pressure was assessed; three reduction ratios were used, namely, 1000, 2500, and 4000. The geometry of the cylindrical die is defined by die reduction ratio, RR = $(D_b/D_a)^2$, die length to diameter ratio (L/D_a), die entrance angle (2α) as shown in Figure 1(a). Dies with three different die land

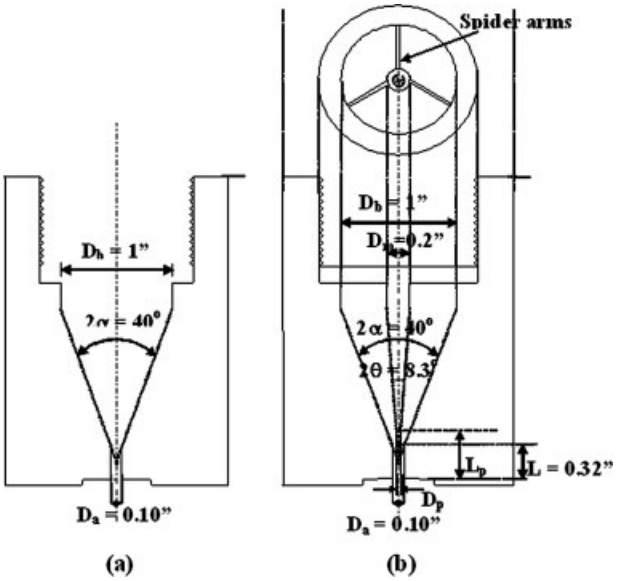

Figure 1 Schematic of (a) Cylindrical die for rod extrusion and (b) annular (cocentric) die for tube extrusion.

diameters (D_a) were used to achieve the reduction ratios of 1000, 2500, and 4000.

PTFE fine powder resin was extruded in a tube shape by using concentric dies. The concentric die comprises of an outer fixture with fixed dimensions shown in Figure 1(b). The main dimensions of the tube die are: entrance angle of $2\alpha = 40^\circ$ and length to diameter ratio, L/D_a. This outer die can accommodate different inserts to produce tubes with different thickness and inner diameter. In this study, two different inserts were used producing reduction ratios, defined by $RR \equiv (D_b^2 - D_m^2)/(D_a^2 - D_p^2)$ of 352 and 1000 as shown in Figure 1(b). A picture of the annular die is seen in Figure 2. The insert is supported on the outer tube by the spider arms [see also Figure 1(b)]. These spider arms provide additional resistance to flow (extra pressure drop) which could not be assessed experimentally. This excess pressure drop due to spider arms will be discussed below when the experimental results are compared with the model predictions.

The extrusion results are presented as extrusion pressure versus apparent shear rate, $\dot{\gamma}_A$. For a cylindrical die, it is defined as $\dot{\gamma}_A \equiv 32Q/\pi D^3$, where Q is the volumetric flow rate and D_a is the diameter of the die at the exit. The apparent shear rate for an annular die, $\dot{\gamma}_{At}$, can be estimated by approximating the tube by a slit die yielding the following expression:

$$\dot{\gamma}_{At} = \frac{6Q}{\pi\left(D_b/2 + D_p/2\right)\left(D_b/2 - D_p/2\right)^2} \quad (1)$$

where D_b is diameter of the capillary and D_p is the diameter of the insert's tip at the exit.

MATHEMATICAL MODELS

The model for PTFE paste flow through cylindrical dies (Ariawan et al.[4]) and annular dies (Patil et al.[14]) is discussed below.

Cylindrical dies

The model which predicts the dependence of extrusion pressure on die geometrical parameters for rod extrusion was developed by Ariawan et al.,[4] based on an earlier development by Snelling and Lontz.[13] Both developments are based on the assumption that the paste obeys the following approximate, one-dimensional constitutive equation:

$$\sigma = C\gamma_{max}^n + \eta\dot{\gamma}_{max}^m \quad (2)$$

where σ is the shear stress, C, η, n, and m are the material parameters and γ_{max}, $\dot{\gamma}_{max}$ denote the maximum strain and strain rate, respectively. Using this constitutive model, Ariawan et al.[4] have derived the following capillary flow model which can be used for rod extrusion:

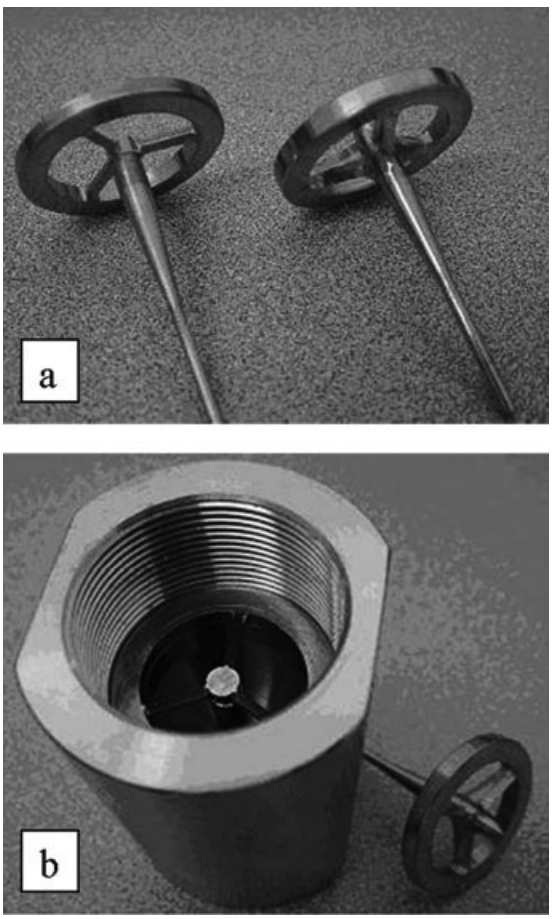

Figure 2 (a) A picture of the two inserts with the spider arms to support them at the inside of the die and (b) The die with the insert inside.

$$P_{\text{rod}} = \sigma_{\text{rb}} = \sigma_{\text{ra}}\text{RR}^{B_1} + 2(1+B_1) \times\left\{C\left(\frac{D_b}{2\sin\alpha}\right)^{2B_1}\int_{a=\frac{D_a}{2\sin\alpha}}^{b=\frac{D_b}{2\sin\alpha}}\frac{(3\ln(r_b/r))^n}{r^{2B+1}}\,dr + \frac{\eta}{(3m+2B)}\left(\frac{12Q\sin^3\alpha}{\pi(1-\cos\alpha)D_b^3}\right)^m(\text{RR}^{B_1+3m/2}-1)\right\}, \quad (3)$$

where P_{rod} is the extrusion pressure through capillary dies [see Fig. 1(a)] f is the friction coefficient, and $B_1 \equiv f\sin\alpha/2(1-\cos\alpha)$. Moreover, the following equations are needed to fully define the model.

$$\sigma_{\text{ra}} = -\sigma_{\text{zo}} = -\text{N}_1(\text{e}^{-4fL/\varepsilon D_a}-1) + \sigma_{\text{zL}}\text{e}^{-4fL/\varepsilon D_a} \quad (4a)$$

$$-N_1 = C\left(\frac{3}{2}\ln(\text{RR})\right)^n + \eta\left(\frac{12Q\sin^3\alpha\text{RR}^{3/2}}{\pi(1-\cos\alpha)D_b^3}\right)^m. \quad (4b)$$

Annular dies

Similarly, Patil et al.[14] have developed a model for tube extrusion in annular dies [see Fig. 1(b)] with a contraction angle of 2α, initial external and internal diameters of D_b and D_m, respectively and final external and internal diameters of D_a and D_p respectively and a land length of L. The same constitutive equation has been used and therefore the material constants C, η, n, and m of Eq. (1) have the same meaning in both capillary and annular flow models. The following tube flow model has been developed by Patil et al.[14]:

$$P_{\text{tube}} = \sigma_{\text{rb}} = \sigma_{\text{ra}}\text{RR}^{B_2} + 2(1+B_2)\left\{C\left(\frac{D_b}{2\sin\alpha}\right)^{2B_2} \times\int_{a=\frac{D_a}{2\sin\alpha}}^{b=\frac{D_b}{2\sin\alpha}}\frac{(3\ln(r_b/r))^n}{r^{2B_2+1}}\,dr + \frac{\eta}{(3m+2B_2)} \times\left(\frac{12Q\sin^3\alpha}{\pi(\cos\Omega-\cos\alpha)D_b^3}\right)^m\left(\text{RR}^{B_2+3m/2}-1\right)\right\}, \quad (5)$$

where the volumetric flow rate for annular dies is $Q \equiv (\pi/4)(D_b^2 - D_m^2)V$, $B_2 \equiv f(\sin\Omega+\sin\alpha)/\,2(\cos\Omega-\cos\alpha)$ and $\Omega = \tan^{-1}(D_m/D_b\tan\alpha)$. Finally, the following two equations are needed to define fully the flow model.

$$\sigma_{\text{ra}} = -\sigma_{\text{zo}} = -N_{1a}(e^{-4fL/\varepsilon D_a}-1) + \sigma_{zL}e^{-4fL/\varepsilon D_a} \quad (6a)$$

$$-N_{1a} = C\left(\frac{3}{2}\ln(\text{RR})\right)^n + \eta\left(\frac{12Q\sin^3\alpha R^{3/2}}{\pi(\cos\Omega-\cos\alpha)D_b^3}\right)^m. \quad (6b)$$

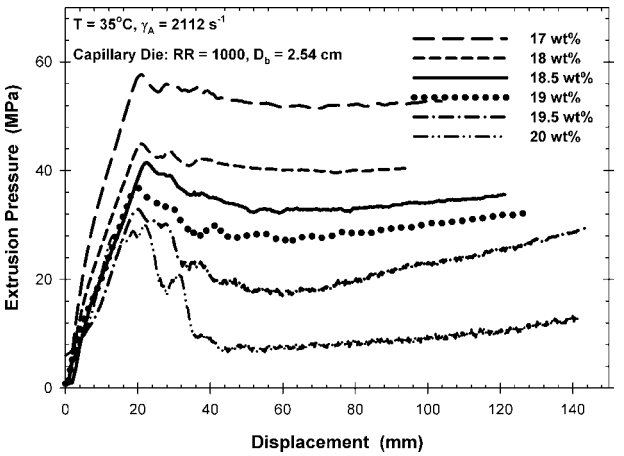

Figure 3 Transient paste extrusion experiments for pastes prepared with resin B containing different lubricant concentration at the shear rate of 2112 s^{-1}.

RESULTS AND DISCUSSION

Paste extrusion through capillary dies

Figure 3 depicts transient paste extrusion experimental runs for pastes prepared with resin B and various concentrations of Isopar® K, namely 17 (36.6), 18 (38.8), 18.5 (40), 19 (41), 19.5 (42), and 20 (43) wt % (vol %) at the apparent shear rate of 2112 s^{-1} using a capillary die. All transients exhibit three zones which have been discussed extensively elsewhere.[16,17] Initially, the pressure increases and goes through a maximum while during this period there is very little flow (zone I). This is due to jamming of the paste at the contraction zone of the die. Once the structure breaks due to applied pressure, flow starts and as a result decreases to its steady-state value (zone II). At the end of the experimental run and due to liquid migration the paste has become relatively dry and as a result the pressure increases slightly (zone III).

The results plotted in Figure 3 indicate that the extrusion pressure is very sensitive to the amount of lubricant concentration. In fact, the extrusion pressure significantly decreases with increase in lubricant concentration. For example, an increase in concentration from 17 (36.6) to 20 (43) wt % (vol %), causes a decrease of pressure from about 50 MPa to about 10 MPa, that is a reduction of 40 MPa (80%). Therefore, it is expected that a small variability of the concentration within experimental error might cause a measurable effect in terms of extrusion pressure. In addition, a higher amount of lubricant makes it difficult to obtain a steady-state pressure due to case of lubricant migration. The steady-state is obtained only over a short period of time for high amount of lubricant. On the other hand, lubricant amounts of 17 (36.6) and 18 (38.8) wt % (vol %) stabilize the extrusion pressure over longer periods of time.

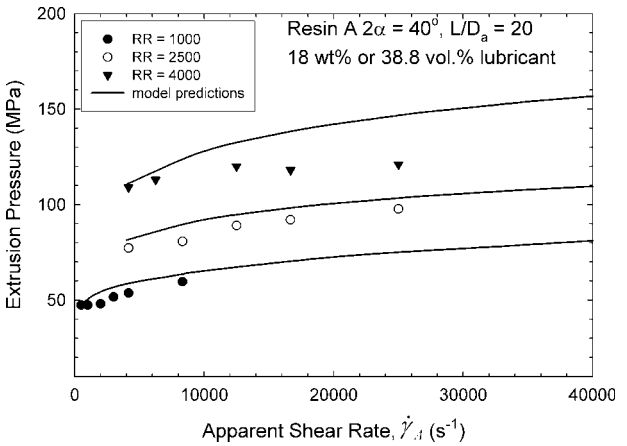

Figure 4 The effect of apparent shear rate on the extrusion pressure of PTFE (Resin A) paste for cylindrical dies having a different reduction ratio (rod extrusion). Solid lines represent the fits of eq. (3).

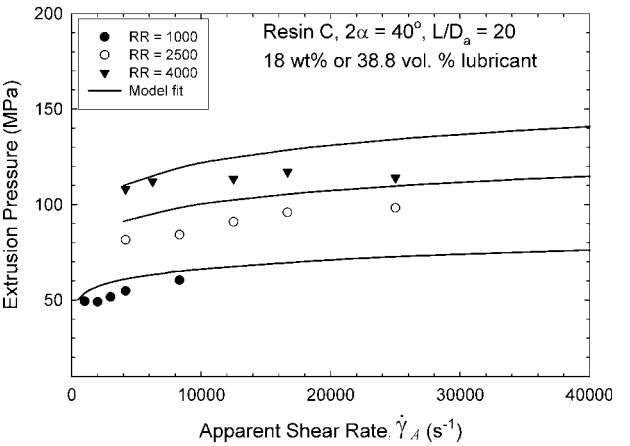

Figure 6 The effect of apparent shear rate on the extrusion pressure of PTFE (Resin C) paste for cylindrical dies having a different reduction ratio (rod extrusion). Solid lines represent the fits of eq. (3).

Figures 4–6 depict the results for the three resins A, B, and C, respectively. The extrusion pressure is reported as a function of the apparent shear rate for three different reduction ratios of RR = 1000, 2000, and 4000. First, the extrusion pressure increases significantly with increase of the reduction ratio, roughly by 50% from 1000 to 2500 and by more than 100% from 1000 to 4000. Resins A and C are extruded at about the same levels of pressure, whereas resin B is extruded at relatively smaller ones. This is due to the higher molecular weight of powder A[4]. The effect of the apparent shear rate on the extrusion pressure is less dramatic and in many cases insignificant.[4,15,16] The lines in Figures 4–6 are model [eq. (3)] fits which are discussed below.

Figure 7 shows the effect of length-diameter ratio, L/D_a, of the die on the extrusion pressure. Dies with different land length were used to extrude the paste. For each die, the paste was extruded at different shear rates and representative results are plotted in Figure 7 for several L/D_a values for all three resins at the apparent shear rate of 8333 s^{-1}. The reduction ratio was kept fixed at 2500 for these cases. The difference in the extrusion pressure between the two groups of resins is evident again. Resins A and C extrude at higher pressures compared to resin B. Similar results were obtained at other apparent shear rate values.

Figure 8 shows the effect of the reduction ratio on extrusion pressure of pastes extruded at the same shear rate of 8333 s^{-1}. It is possible to see how the extrusion pressure increases nonlinearly with an increase in the reduction ratio at a given apparent shear rate. The same picture is obtained for many other values of the apparent shear rate. As discussed

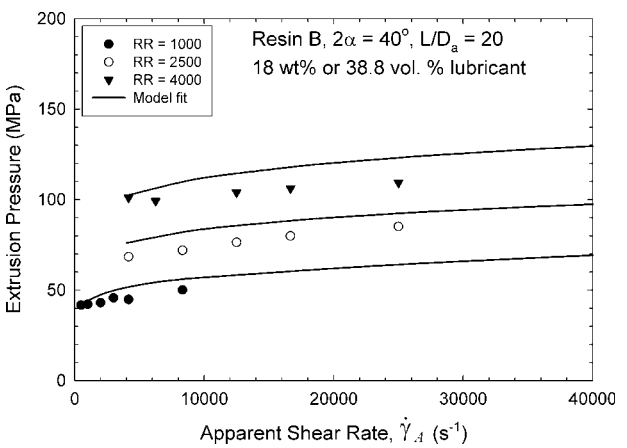

Figure 5 The effect of apparent shear rate on the extrusion pressure of PTFE (Resin B) paste for cylindrical dies having a different reduction ratio (rod extrusion). Solid lines represent the fits of eq. (3).

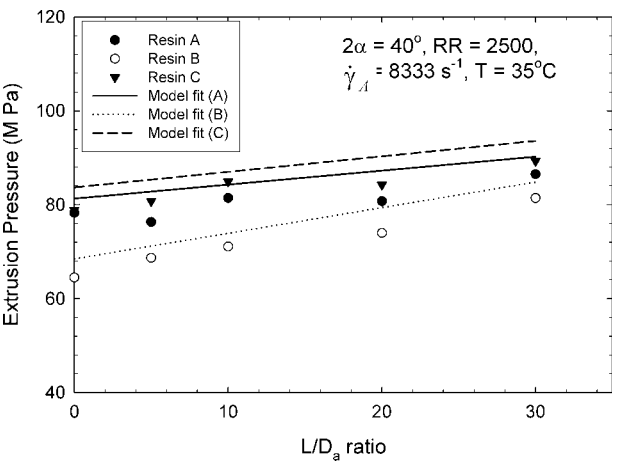

Figure 7 The Effect of L/D_a ratio on the extrusion pressure of pastes prepared with different resins and extruded at the apparent shear rate of 8333 s^{-1} (rod extrusion). Continuous lines represent the fits of eq. (3).

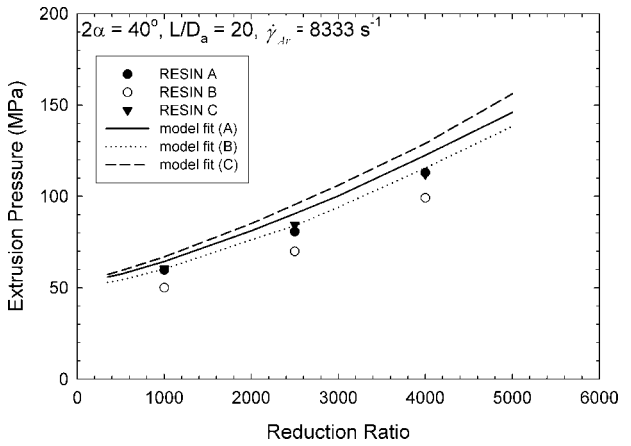

Figure 8 Effect of reduction ratio on the extrusion pressure of paste prepared with different resins and extruded at an apparent shear rate of 8333 s^{-1} (rod extrusion). Continuous lines represent the fits of eq. (3).

earlier, the continuous lines represent model [Eq. (3)] fits to the experimental data.

Paste extrusion through annular dies

Figures 9 and 10 plot the extrusion pressure for resin A, B, and C in tube extrusion for reduction ratios of 352 and 1000, respectively, at a given L/D_a ratio of 20 and contraction angle of 40° for several apparent shear rate values. The effect of apparent shear rate on the extrusion pressure is small. The small decrease of extrusion pressure at small apparent shear rates (Fig. 9) is due to lubricant migration which is facilitated due to long times of extrusion. Resins A and C extrude at higher pressures compared to resin B as was the case in the extrusion through capillary dies. Moreover, the extrusion pressure in annular dies is considerably higher than those in capillary at given L/D_a ratio, apparent shear rate, reduction ratio, and contraction angle. The continuous lines are model [eq. (5)] predictions as opposed to the lines in Figures 4–7 which are model fits. This is discussed in the following section.

Model predictions and comparison with experiments

In this section, the models for paste extrusion through capillary and annular dies, that is eqs. (3) and (5), respectively, are compared with the available experimental results. Both models are based on the ''approximate,'' one dimensional constitutive Eq. (2) and therefore, include the same material parameters. The idea is to first fit the model parameters using the experimental data for the extrusion through capillary dies and then use the parameters to predict the extrusion pressure through annular dies. The dependence of the extrusion pressure on the apparent shear rate, the die entrance angle (2α), and the die reduction ratio (RR) will be discussed in detail to demonstrate the consistency of the models.

The material parameters C, n, η, m, and f of eq. (3) are evaluated by fitting the model to experimental data for resins A, B and C plotted in Figures 4–7. In fact more data have been used not presented here for the sake of simplicity. The calculated model parameters C, n, η, m and f are determined by nonlinear dynamic optimization using a Gauss-Newton iterative algorithm that minimizes the objective function. The objective function in the present study has a form of:

$$\mathrm{SSE} = \frac{1}{N}\sum_{i=1}^{N}\left(\frac{P_{\mathrm{exp}} - P_{\mathrm{calc}}}{P_{\mathrm{exp}}}\right)^2 \tag{7}$$

where SSE is the sum of squares error.

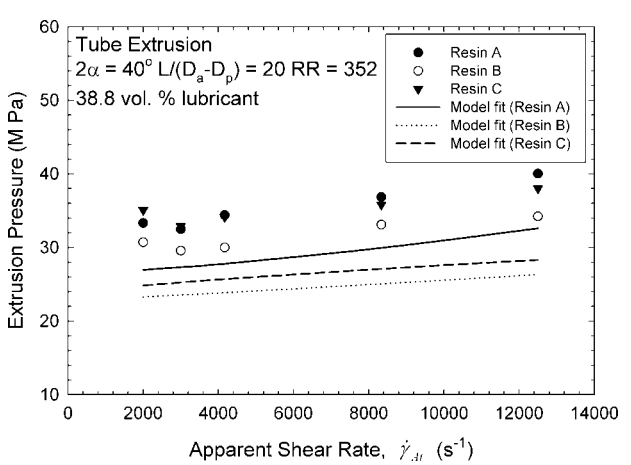

Figure 9 The effect of apparent shear rate on the extrusion pressure of three PTFE pastes extruded through an annular die having a reduction ratio of 352 (tube extrusion). Continuous lines represent the fits of eq. (5).

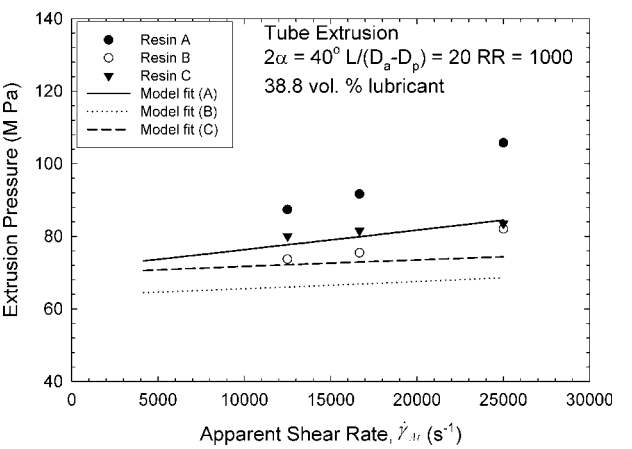

Figure 10 The effect of apparent shear rate on the extrusion pressure of three PTFE pastes extruded through an annular die having a reduction ratio of 1000 (tube extrusion). The continuous lines represent the predictions of eq. (5).

TABLE II
Values of Material Constants and Coefficient of Friction Needed in Eq. (3) to Predict the Extrusion Pressure for Paste Flow in Cylindrical and Annular Dies

Resin	C (MPa)	n	η (MPa s)	m	f
Resin A	1.26×10^{-1}	2.31	1.34×10^{-3}	1.36	0.01013
Resin B	9.81×10^{-2}	2.26	4.06×10^{-3}	1.22	0.0193
Resin C	1.11×10^{-2}	2.15	7.68×10^{-4}	0.91	0.0281

The values of the parameters are listed in Table II for the three resins. To make sure that the global minimum has been achieved during nonlinear parameter estimation, the sensitivity analysis is performed.[18] Sensitivity analysis is applied to each of the five estimated parameters by means of perturbation of the parameter value (keeping the other parameters in their estimated values). Perturbations are preferable done in the range of ± 20%. For each perturbation in the parameter values the objective function is reevaluated and then for each parameter the perturbation percentage is plotted against the corresponding value of the objective function. If all perturbations in all the parameters give the minimum of the objective function with their original values (0% perturbations), then the global minimum has been achieved. On the contrary, if at least one parameter does not give the same minimum as the others at 0% perturbation, that means poor nonlinear parameter estimation. In the present study, it is clearly seen from Figure 11 that the estimated parameters are the optimum since at 0% perturbation the SSE is the minimum. It is also seen that the model predictions are very sensitive to parameters n and m as compared to C, η, and f.

Overall, the model describes the data reasonably well both quantitatively and qualitatively predicting the correct trends. These trends include increase of pressure with increase of apparent shear rate, L/D_a ratio, and reduction ratio. The model predicts correctly the nonmonotonic variation of pressure with contraction ratio (existence of a minimum at contraction angles between 20° and 40° depending on the resin), a trend not presented here as this has been published and discussed extensively elsewhere.[4,14,16]

Figures 9 and 10 depict the extrusion pressure for resins A, B, and C in tube extrusion for reduction ratios of 352 and 1000, respectively. The lines indicate model predictions for tube extrusion using the model parameters calculated before. As expected, the extrusion pressure in annular dies is higher than in cylindrical dies under comparable conditions. This is mainly due to the presence of the additional wall surface area within the annular die. The model overall under predicts the experimental data in all cases although as will be discussed here the predicted trends are correct. One reason for the under prediction is that the experimental data includes the additional excess pressure due to the presence of the spider arms (see Fig. 2). This additional pressure drop could not be assessed independently.

Figure 12 shows the model predictions for the dependence of extrusion pressure on the die reduction ratio for annular die using the parameters for the three resins. The reduction ratio of the die is increased by decreasing the diameters D_a and D_p for the annular die. The nonlinear dependence of extrusion pressure on the die reduction ratio is clearly seen from the model predictions; however similar behavior could not be confirmed from the experiments due to lack of experimental data.

Finally, Figure 13 compares the model prediction with experimental results for the dependence of the extrusion pressure on the die $L/(D_a - D_p)$ ratio in the case of annular dies. The extrusion pressure linearly

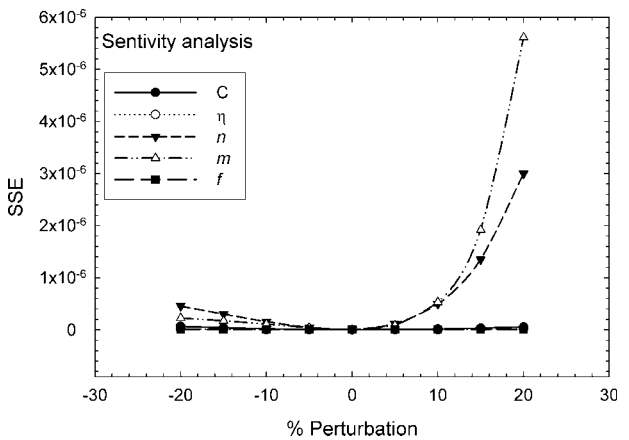

Figure 11 Sensitivity analysis of estimated parameters for the rod extrusion model [eq. (5)].

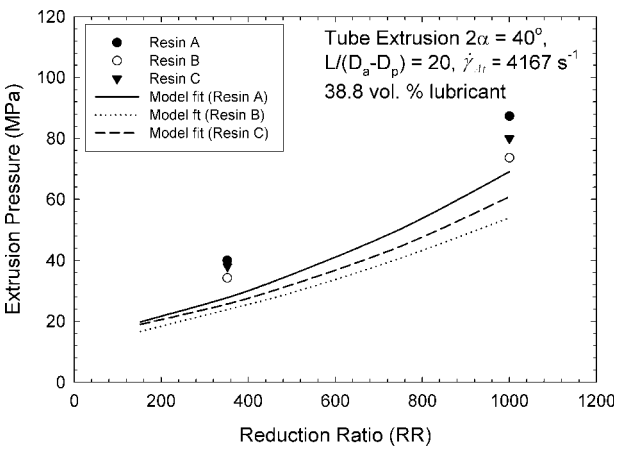

Figure 12 The effect of the die reduction ratio (RR) on the extrusion pressure of three PTFE pastes extruded through annular dies of two different reduction ratios (tube extrusion). Continuous lines represent the fits of eq. (5).

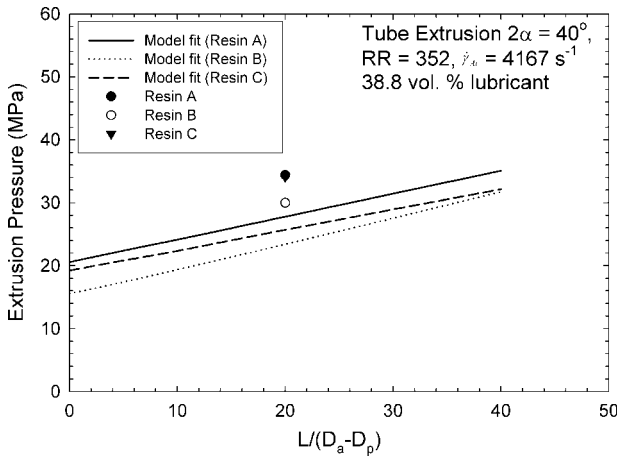

Figure 13 The effect of die length-to-diameter ratio, $L/(D_a - D_p)$, on the extrusion pressure of three PTFE pastes extruded through an annular die having an $L/(D_a - D_p) = 20$ (tube extrusion). Continuous lines represent the fits of Eq. (5).

increases with $L/(D_a - D_p)$ ratio as shown in Figure 13 with almost the same trend for all resins (similar dependence in the case of capillary dies, see Fig. 7). Note the small value of the friction factor, f, which implies that the pressure drop in the die land is much smaller compared to that in the conical zone. This is reasonable due to the presence of the lubricant. Most of the resistance to flow occurs in the contraction area. In spite of the presence of lubricant at the solid walls, considerable energy is consumed in the deformation of the paste elements as they accelerate given that the presence of fibrils contribute tremendously in this deformation.

Overall the agreement between the model predictions and experimental analysis is good, and indicates that the model of eqs. (3) and (5) can be used to describe paste extrusion in both cylindrical and annular dies.

CONCLUSIONS

The paste extrusion behavior of three PTFE powders at high reduction ratios was examined using both capillary and annular dies having a variety of geometrical characteristics such as length-to diameter ratios, and reduction ratio. Based on these experimental results, the validity of a flow model for tube paste extrusion proposed by Patil et al.[14] was demonstrated. First, the model for rod extrusion proposed by Ariawan et al.[4] was used to determine the material parameters by fitting the model to experimental results. Consequently, the predictions of the tube extrusion model proposed by Patil et al.,[14] were compared with experimental data. It was demonstrated that the model successfully predicts at least qualitatively and to a certain extent quantitatively the dependence of extrusion pressure on apparent shear rate, reduction ratio and length-to-diameter ratio of the annular die.

A final comment relates to the limitations of this analytical model. While the extrusion pressure can be predicted well as a function of the operating parameters and the geometrical characteristics of the dies, the material's structure (fraction of fibrillated domains), is not explicitly calculated. For these cases, a numerical algorithm and the use of a more sophisticated flow model has been proposed in the literature.[19]

NOMENCLATURE

B_1	model parameter defined as $f \sin\alpha/2(1-\cos\alpha)$
B_2	model parameter defined as $f(\sin\Omega + \sin\alpha)/2(\cos\Omega - \cos\alpha)$
C	proportionality constant for the elastic term in eq. (2), Ludwik's power law model[20]
D_a	die exit diameter
D_b	die entrance diameter
D_m	mandrel diameter at the inlet of the annular die
D_p	mandrel diameter at the exit of the annular die
E	Young's modulus of elasticity
f	Coulomb's law coefficient of friction, between PTFE paste and die wall
L	length of die land
m	power law index for the viscous term of the eqs. (3) and (5)
n	power law indices for the elastic term of eqs. (3) and (5)
N_1, N_{1a}	first normal stress difference. N_{1a} is the first normal stress difference calculated at the exit of the die
$P_{\text{Extrusion}}$	Extrusion Pressure
P_{rod}	rod extrusion pressure
P_{rod}	tube extrusion pressure
Q	volumetric flow rate.
RFH	''radial flow'' hypothesis
RR	die cross-sectional reduction (contraction) ratio
SSE	sum of squares error
T	time

Hellenic characters

α	half die entrance angle
$\dot{\gamma}_{\text{At}}$	apparent shear rate for tube extrusion
$\dot{\gamma}_A$	apparent shear rate
$\gamma_{\max}, \dot{\gamma}_{\max}$	maximum strain and strain rate, respectively. Maximum strain is defined as the difference of strains in the first two principal directions

$\varepsilon, \dot{\varepsilon}$	strain and strain rate, respectively
η	viscosity coefficient
σ	total stress
σ_{ra}	stress at the exit of the conical section of the die
σ_{zo}	stress at the entrance of the die land
σ_{zL}	stress at the exit of the die land

References

1. Mazur, S. In Polymer Powder Technology; Narkis, M., Rosenzweig, N., Eds.; Marcel Dekker: New York; Chapter 9, 1995.
2. Ebnesajjad, S. Fluoroplastics, Vol. 1: Non-Melt Processible Fluoroplastics; William Andrew Corp: New York, 2000.
3. Benbow, J. J.; Bridgwater, J. Paste Flow and Extrusion; Oxford University Press: Oxford, 1993.
4. Ariawan, A. B.; Ebnesajjad, S.; Hatzikiriakos, S. G. Can J Chem Eng 2002, 80, 1153.
5. Larson, R. Constitutive Equations for Polymer Melts and Solutions; Butterworths: Boston, 1998.
6. Hoffman, O.; Sachs, G. Introduction to the Theory of Plasticity for Engineers; McGraw-Hill Company: New York, 1953.
7. Davis, E. A; Dukos, J. J Appl Mech 1994, 11, 193.
8. Benbow, J. J.; Oxley, E. W.; Bridgwater, J. Chem Eng Sci 1987, 42, 2151.
9. Benbow, J. J.; Bridgwater, J. Chem Eng Sci 1987, 42, 735.
10. Benbow, J. J.; Lawson, T. A.; Oxley, E. W.; Bridgwater, J. Ceram Bull 1989, 68, 1821.
11. Dealy, J. M.; Wissbrun, K. F. Melt Rheology and its Role in Plastics Processing: Theory and Applications; Van Nostrand Reinhold: New York, 1990.
12. Basterfield, R. A.; Lawrence, C. J.; Adams, M. J. Chem Eng Sci 2005, 60, 2599.
13. Snelling, G. R.; Lontz, J. F. J Appl Polym Sci 1960, 3, 257.
14. Patil, P. D.; Feng, J. J.; Hatzikiriakos, S. G. AIChE J 2006, 52, 4028.
15. Ochoa, I.; Hatzikiriakos, S. G. Powder Technol 2004, 146, 73.
16. Ochoa, I.; Hatzikiriakos, S. G. Powder Technol 2005, 153, 108.
17. Ochoa, I.; Hatzikiriakos, S. G.; Mitsoulis, E. Int Polym Proc 2006, XXI, 497.
18. Verma, A.; Morbidelli, H.; Wu, H. Parametric Sensitivity in Chemical Systems, 1st ed.; Cambridge Series in Chemical Engineering: UK, 1999
19. Patil, P. D.; Feng, J.; Hatzikiriakos, S. G. J Non-Newtonian Fluid Mech 2006, 139, 44.
20. Ludwik, P. Elemente der Technologischen Mechanik; Springer-Verlag: Berlin, 1909.